Thin Film Morphology of Symmetric Semicrystalline Oxyethylene/Oxybutylene Diblock Copolymers on Silicon

Guo-Dong Liang, Jun-Ting Xu,* and Zhi-Qiang Fan

Key Laboratory of Macromolecular Synthesis and Functionalization, Department of Polymer Science & Engineering, Zhejiang University, Hangzhou 310027, China

Shao-Min Mai and Anthony J. Ryan

Department of Chemistry, The University of Sheffield, S3 7HF, Sheffield, U.K.

Received February 23, 2006; Revised Manuscript Received April 24, 2006

ABSTRACT: Thin film morphologies of four symmetric semicrystalline oxyethylene/oxybutylene diblock copolymers ($E_{76}B_{38}$, $E_{114}B_{56}$, $E_{155}B_{76}$, and $E_{224}B_{113}$) were investigated by tapping mode atomic force microscopy (AFM). The effects of chain length, annealing, and surface property were examined. It is found that the lamellar orientation of the nascent block copolymer thin film varies with chain length. For low molar mass block copolymers ($E_{76}B_{38}$, $E_{114}B_{56}$, and $E_{155}B_{76}$), the lamellar orientation is parallel to the silicon surface, but for the high molar mass block copolymer, $E_{224}B_{113}$, the lamellar orientation is perpendicular to the silicon surface. The nascent block copolymer thin films of the low molar mass block copolymers are composed of multiple polymer layers with mixed thicknesses $L \approx L_0$ and $L \approx {}^1/_2L_0$, where L_0 is the long period of the block copolymers in the bulk. The existence of polymer layers with $L \approx {}^1/_2L_0$ besides the first layer on the substrate surface indicates that the crystalline domain consists of double crystalline layers, and parts of the poly(oxyethylene) block can also be located at the polymer/air interface. Annealing leads to the disappearance of the metastable polymer layer of thickness $L \approx L_0/2$ via a morphological transformation involving different polymer layers and slight increase in lamellar thickness. The heterogeneities on the substrate surface can nucleate crystallization of block copolymer thin film during annealing when the lamellar structure is perpendicular to the surface, leading to formation of spherulites. The silicon surface was modified by grafting a monolayer of hydrophobic silane. On the modified surface, the lamellar structure of $E_{224}B_{113}$ becomes parallel to the surface, and the nucleation effect of the heterogeneities on crystallization of poly(oxyethylene) block is suppressed.

Introduction

Block copolymer thin films have attracted increasing attention because of their potential technological applications such as lithographic masks and photonic materials.[1−4] Block copolymer thin film is often characterized by highly oriented domains, which are the direct result of minimization in surface and interface energy. Lamellar structures with orientation both parallel and perpendicular to the substrate surface can be formed in symmetric block copolymer thin films. For lamellar structures parallel to the substrate surface, the morphology develops through the surface and substrate boundary condition that demands the most energetically compatible block to be expressed at each surface. In the systems with a small surface free energy difference ($\Delta\gamma$) and a high degree of microphase separation, formation of thin films with lamellar structure perpendicular to the substrate surface is also possible.[1]

Crystallization can also be viewed as one of the driving forces of self-assembly. When combined with microphase separation and surface tension, crystallization can be used to control thin film morphology of semicrystalline block copolymers.[5−8] However, formation of thin film structure of semicrystalline block copolymers is very complicated. First, polymer crystallizes in a confined two-dimensional space in the thin film.[9,10] Under such circumstance, crystallization processes and the final morphology of semicrystalline block copolymer may be quite different from that in bulk due to the contributions of surface energy and two-dimensional confinement. Second, not only orientation of the lamellar structure but also orientation of crystal stems needs to be considered. Some authors have reported thin film morphology of semicrystalline block copolymers, including orientation of microphase-separated domain at large scale,[9,11−13] registration of crystalline stems,[14−16] nucleation mechanism and growth kinetics,[17−19] and morphological reorganization.[20,21] It has also been shown that the thin film morphology of semicrystalline block copolymers strongly depends on crystallization conditions such as thermal history, solvent, and annealing.[19,22−25]

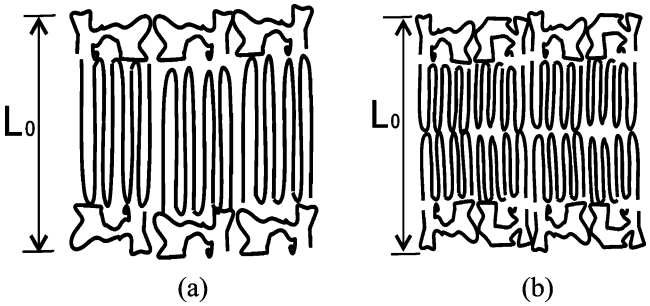

Figure 1. Two model structures for semicrystalline diblock copolymers.

Despite the work mentioned above, there are still some unresolved problems in thin films of semicrystalline block copolymers. There are at least two possible structures for thin film of semicrystalline block copolymers, as shown in Figure 1:[14,26−28] one containing single crystalline layer and the other containing double crystalline layers. These two structures are difficult to distinguish. In the literature, both structure models are adopted by different authors, but generally no direct evidence

* Corresponding author: Fax +86-571-87952400; e-mail xujt@zju.edu.cn.

10.1021/ma060405p CCC: $33.50
Published on Web 07/06/2006

is presented.[14,26−28] Moreover, it has been found the relative segregation strength, expressed as the ratio $\chi N/\chi N_{ODT}$ (where χ is the Flory−Huggins interaction parameter and N is the degree of polymerization), has a tremendous influence on crystallization and morphology of block copolymers in bulk.[29,30] Similarly, cylinder and lamellar orientation in thin films of amorphous block copolymer also depends on molecular weight (a segregation strength effect).[31] But so far the effect of segregation strength on thin film morphology of semicrystalline block copolymer is rarely reported.[28] Herein we study the thin film morphology of four symmetric oxyethylene/oxybutylene diblock copolymers with different chain lengths. Since large segregation strength together with two-dimensional thin film morphology acts as a strong confinement on crystallization[20,21,32] and reduces the variation in morphology, we chose a series of semicrystalline block copolymers with different segregation strengths. When crystallization temperature is constant, the relative segregation strength $\chi N/\chi N_{ODT}$ is approximately expressed by the degree of polymerization, as χN_{ODT} is invariant. As anticipated, different thin film morphologies can be obtained by regulating the relative strength of crystallization, surface tension, and segregation of the two unlike blocks; hence, the effects of annealing and modification of substrate surface on thin film morphology were also investigated. The results show that the orientation of the microphase-separated structure strongly depends on chain length and surface property. It is also shown that microphase segregation strength, crystallization condition, and surface property can be used to regulate the morphology of semicrystalline block copolymers.

Experimental Section

Materials. The synthesis and characterization of oxyethylene/oxybutylene block copolymers, $E_{76}B_{38}$, $E_{114}B_{56}$, $E_{155}B_{76}$, and $E_{224}B_{113}$ (where E and B denote oxyethylene and oxybutylene units, respectively, and denoted as E_mB_n, where the subscripts refer to the average degree of polymerization), have been described elsewhere.[33−35] All the block copolymers have narrow molecular weight distributions ($M_w/M_n < 1.05$) by GPC and have a lamellar morphology in both the solid and liquid bulk phases. Parameters of the block copolymers are summarized in Table 1. The single-crystal silicon wafers (p-type, 6 in. diameter) were supplied by Shanghai Institute of Ceramics, China. They were cut into chips of about 10 mm × 10 mm in size and then treated with "piranha" solution, a mixture of 70 vol % concentrated sulfuric acid and 30 vol % hydrogen peroxide, for about 30 min at 60 °C to generate a clean, hydrophilic oxide surface. The substrate was then rinsed with a large volume of distilled water and dried in a vacuum oven at 80 °C for 8 h.

Modification of Silicon Surface. The vapor phase method was chosen to modify silicon wafers, which can induce the formation of monolayer silane film on a solid surface bearing hydroxyl groups. Some silicon chips about 10 mm × 10 mm in size were stuck to plastic plates, and then ~5 mL of trimethylchlorosilane was deposited in a 50 mL plastic jar. The plastic plates were placed on the jar, mounted so that the fresh surface faced the silane liquid. After the jar was settled into a vacuum desiccator, the desiccator was evacuated to 10 Torr. The substrates were then allowed to react with the silane vapor for 5 h at room temperature. After the substrates were rinsed ultrasonically with dry toluene and then ethanol for 10 min, they were cured at 120 °C for 3 h in an oven under ambient pressure.

Preparation of Diblock Copolymer Thin Films. Block copolymer thin films were prepared by spin-coating 0.5% w/v E_mB_n dichloromethane solutions on silicon wafers. Solvent was allowed to evaporate simultaneously during the spin-coating process. Annealing of diblock copolymer thin films was conducted at 35 °C in a vacuum system (10 Torr). After annealing of diblock copolymer thin films, AFM was conducted immediately.

Table 1. Parameters of E_mB_n Diblock Copolymers

copolymers	ϕ_E[a] (solid state)	w_E[b] (solid state)	long period in bulk L_0 (nm)	T_c (°C)[c]	$N\chi$[d]
$E_{76}B_{38}$	0.49	0.55	16.7	35	19.9
$E_{114}B_{56}$	0.50	0.55	19.8	38	29.7
$E_{155}B_{76}$	0.50	0.56	22.0	40	40.4
$E_{224}B_{113}$	0.49	0.55	33.3	43	58.9

[a] $\phi_E = m/[m + (72/44)(1.23/0.97)n]$, ϕ_E = the volume fraction of the E block, 1.23 g/cm^3 being the density of E in the crystalline state and 0.97 g/cm^3 the density of B in the liquid state, both at 20 °C. [b] $w_E = m/[m + (72/44)n]$, w_E = the weight fraction of the E block. [c] T_c: at cooling rate of 10 °C/min. [d] χ: calculated for E_mB_n diblock copolymer bulk at 20 °C.

Water Contact Angle Measurement. The axisymmetric drop shape analysis profile was used to determine the contact angles from the shape of axisymmetric sessile drops. The strategy used is to fit the shape of experimental drops to the theoretical drop profile according to the Laplace equation of capillarity. The water contact angle method is employed to determine hydrophilicity of substrates such as silicon and modified silicon wafers. At least 10 values were obtained for each substrate sample.

Atomic Force Microscopy (AFM). The thin film morphology of E_mB_n block copolymers was investigated by atomic force microscopy (SPA 300HV/SPI3800N Probe Station, Seiko Instruments Inc., Japan) in the tapping mode. A silicon microcantilever with a spring constant 16 N/m and resonance frequency ~138 kHz was used. The scan rate ranged from 0.5 to 2.0 Hz to optimize the quality of AFM image. The set-point ratio, the ratio between the set-point amplitude and the free vibration amplitude (the lowest amplitude when tip and sample are not in contact), was chosen to be ~0.8. Parameters characterizing features of thin film such as thickness of lamellar and difference of phase shift were obtained directly from cross-sectional profiles. To ensure the repeatability of the data, cross-sectional profiles from different area of height or phase images were necessary. At least 10 values were obtained for each parameter.

Grazing Incidence X-ray Diffraction (GIXRD). Grazing incidence techniques were carried out to investigate the crystal structure of diblock copolymer thin film at room temperature. A BEDE D1 high-resolution X-ray diffractometer, equipped with a Cu Kα radiation source was used. The diffracted beam is in the plane defined by the incidence beam and the surface normal. This geometry is sensitive to the structure parallel to the surface. Different grazing incidence angles were tested, and better contrast of diblock copolymer signal over silicon signal with smaller error induced by surface undulation at the same time was obtained at grazing incidence angle of 0.6°. The XRD curves were scanned in the 2θ range of 3.0°−30°.

Results and Discussion

Morphology of the As-Spun, Nascent Thin Films. The structure of the as-spun, or nascent, thin films provides an insight into the structure of the polymer as it orders by solvent evaporation during spinning. Figure 2a shows the height image of the nascent $E_{76}B_{38}$ thin film spin-coated from dichloromethane solution at a concentration of 0.5% w/v. Although the morphology of diblock copolymer thin film obtained this way is metastable, it is important to investigate the initial segregation behavior of diblock copolymers in thin film.[31] Height images show that the film is composed of multiple polymer layers, with some bare silicon substrate, and there is periodicity in the direction perpendicular to the substrate surface. An image with higher magnification reveals no ordered structure within the polymer layers, and the AFM images are not presented here. By inference, the lamellar structure of $E_{76}B_{38}$ is parallel to the surface of silicon wafer. Such a morphology is not out of our expectation, since the surface of silicon is covered with hydroxyl groups and inclines to absorb hydrophilic oxyethylene segments in the block copolymer. Similar results have been reported for

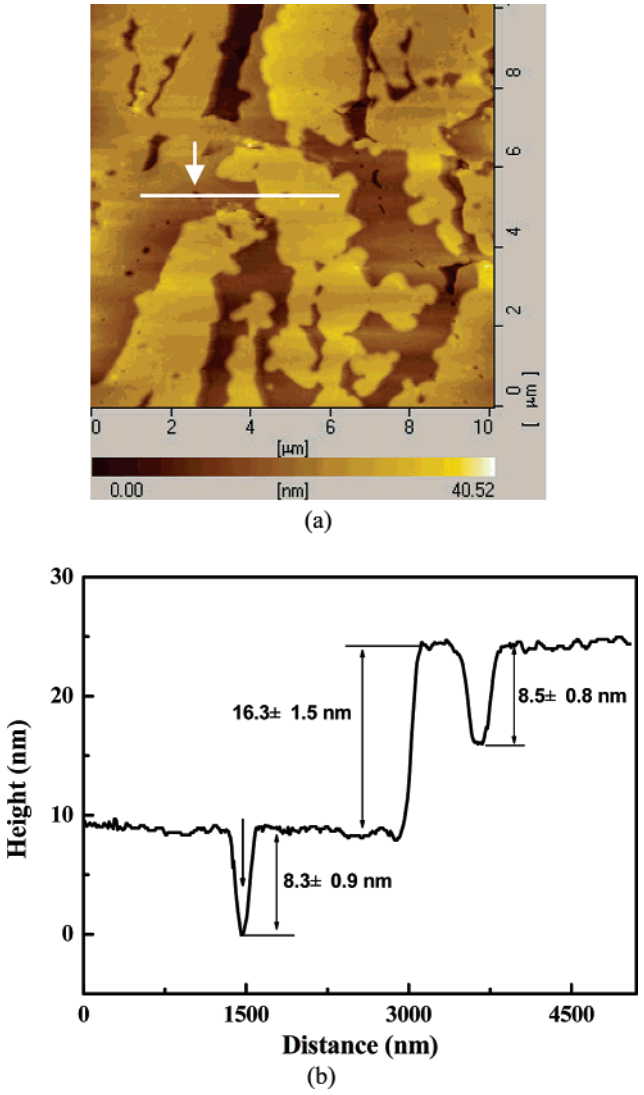

Figure 2. Tapping mode AFM height image and cross-sectional profile of nascent $E_{76}B_{38}$ thin film on silicon spin-coated from solution at concentration of 0.5% w/v: (a) height image; (b) cross-sectional profile. The arrow indicates the hole throughout thin film, confirmed by the sharp difference in phase shift between silicon and polymer surfaces.

thin films of asymmetric oxyethylene/oxybutylene diblock and triblock copolymer with short chain lengths.[36] Comparing the height of the nascent block polymer thin film with the long periods of the amorphous and crystallized block copolymers in bulk, we can draw the conclusion that the E block in the nascent thin film is crystalline. For example, the step change in height of the nascent $E_{76}B_{38}$ thin film is 8.3 ± 0.9 or 16.3 ± 1.5 nm, which is half of or equal to the long period of crystallized $E_{76}B_{38}$ in bulk (16.7 nm),[37] whereas the long period of amorphous $E_{76}B_{38}$ in bulk at 35 °C is only 11.4 nm.[37]

As can be seen from Figure 2a, not all the surface of the substrate is covered by the semicrystalline block copolymer and there are some irregular holes. The cross-sectional profile (Figure 2b) reveals that nearby the holes the average thickness of the first layer of block polymer on the substrate is 8.3 ± 0.9 nm, about half of the long period (L_0) of the crystallized block copolymer in bulk.[37] Apart from the first layer of block polymer on the substrate, we also observe some polymer layers of $L_0/2$ height together with the layers of L_0 height. A similar phenomenon was also observed in the nascent $E_{114}B_{56}$ and $E_{155}B_{76}$ thin films on silicon (see Supporting Information). In the multiple-layer thin film of amorphous or semicrystalline

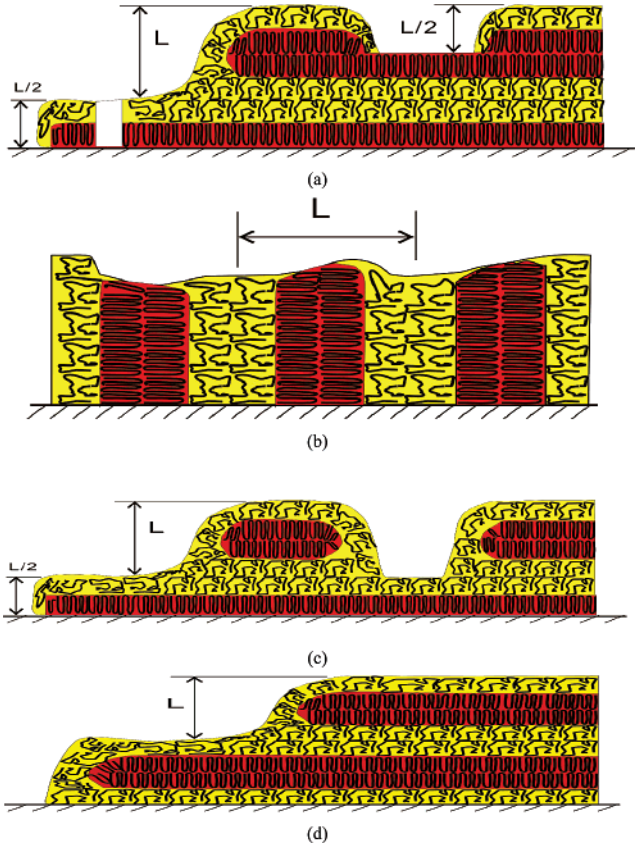

Figure 3. Schematic structures for nascent $E_{76}B_{38}$ thin film on silicon (a), nascent $E_{224}B_{113}$ thin film on silicon (b), annealed thin film of $E_{76}B_{38}$ on silicon (c), and nascent $E_{224}B_{113}$ thin film on modified silicon (d).

block copolymers with asymmetric interfaces, usually only the first layer on the substrate surface has the thickness of $L \approx {}^1/_2L_0$, but the other layers have thicknesses of $L \approx L_0$.[1−3,31] The existence of a polymer layer with thickness of $L_0/2$ besides the first layer on the substrate shows that the crystalline domain in the block copolymer consists of double crystalline layers (corresponding to structure b in Figure 1), and the poly(oxyethylene) block can also be located at the air/polymer interface. As a result, here we present a direct evidence for the structure of crystalline domain in crystalline block copolymers. The thin film structure of $E_{76}B_{38}$ can be schematically depicted as in Figure 3a. Only by stacking in this way can displacement happen to the two adjacent crystalline layers or amorphous layer, leading to the polymer layers with thickness $L = {}^1/_2L_0$ besides the first polymer layer on the substrate. It is established that the oxybutylene blocks with alkyl groups have lower surface energy and tend to enrich at the air/polymer interface. However, in such a morphology, parts of polyoxyethylene blocks are inevitably also located at the air/polymer interface, possibly because oxyethylene and oxybutylene units have so little difference in their surface free energies. Moreover, before crystallization both blocks have high mobility, so parts of poly(oxyethylene) segments can also locate at the air/polymer interface. After crystallization these parts of poly(oxyethylene) segments are temporarily solidified on the air/polymer interface.

The nascent thin films of $E_{114}B_{56}$ and $E_{155}B_{76}$ also exhibit a lamellar structure parallel to the surface (see Supporting Information). However, with further increase in chain length, the situation becomes quite different. Figure 4 shows AFM images of a nascent thin film of $E_{224}B_{113}$ on silicon. Image analysis shows that there is no characteristic periodicity in the direction perpendicular to substrate surface, but stripelike

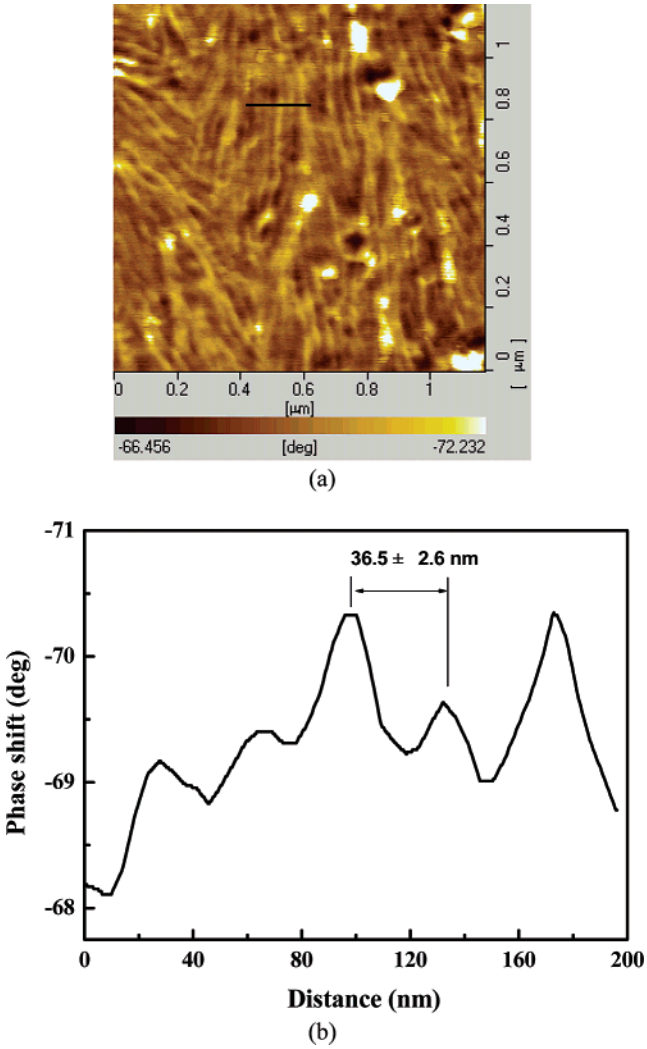

Figure 4. Tapping mode AFM phase image and cross-sectional profiles of nascent $E_{224}B_{113}$ thin film on silicon spin-coated from solution at concentration of 0.5% w/v: (a) phase image; (b) cross-sectional profile along the line in (a).

lamellar texture is observed in the phase image with higher magnification, and this block copolymer exhibits periodicity in the direction parallel to the substrate surface, indicating that there is a lamellar structure perpendicular to the substrate surface in $E_{224}B_{113}$. The periodicity is about 36.5 nm, which is slightly larger than the long period of crystallized $E_{224}B_{113}$ in bulk (33.3 nm). As a result, a thin film of $E_{224}B_{113}$ exhibits a lamellar orientation perpendicular to the silicon surface, as shown in Figure 3b. The change of thin film morphology of E_mB_n block copolymers with chain length shows that lamellar orientation parallel to the substrate surface is preferable for the diblock copolymers with low molar mass, and lamellar orientation perpendicular to the substrate surface is preferable for the diblock copolymers with high molar mass. A similar transformation of lamellar orientation induced by molecular weight was also reported for amorphous block copolymers.[31] Indeed, this change could be simply a relic of the morphology of the block copolymer melt (or concentrated solution). During the spin-coating process the polymer solution becomes progressively more concentrated; at some critical concentration the block copolymer forms an ordered lamellar phase, and as the solution becomes more concentrated the E block starts to crystallize. It is highly likely that the lamellar orientation developed in the initial ordering process is retained during the rapid crystallization process at room temperature, even though crystallization is

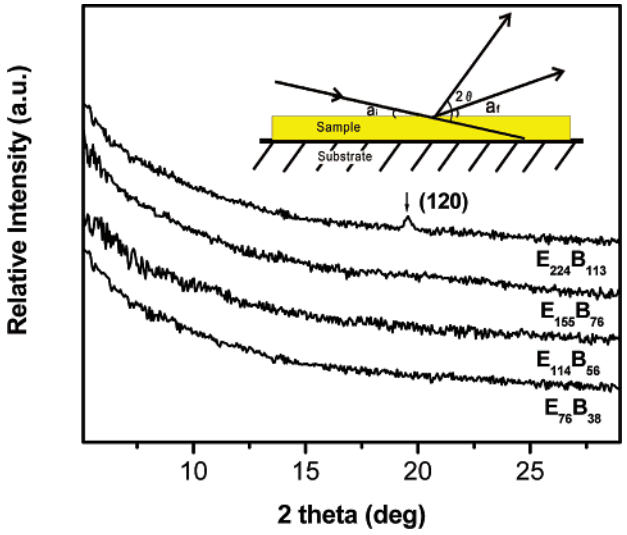

Figure 5. GIXRD patterns of nascent E_mB_n thin film on silicon spin-coated from solution at concentration of 0.5% w/v.

normally associated with an increase in lamellar spacing.[37] Thus, the nascent structure of the as-spun polymer film may well reflect the morphology of the preceding polymer melt.

When the lamellar structure is perpendicular to the substrate surface, there is usually a large contrast in the phase image. However, we notice a small difference in the phase angle in Figure 4a. This may be due to the lower crystallinity of the poly(oxyethylene) block and smaller difference in viscoelasticity between these two blocks in the nascent E_mB_n thin film. Indeed, after a long annealing time the crystallinity of the poly(oxyethylene) block is enhanced, and a larger shift in the phase image is observed.

Figure 5 shows the grazing incidence X-ray diffraction (GIXRD) curves of E_mB_n thin films. The inset shows the schematic graph of GIXRD. The grazing incidence angle is set to be 0.6°. According to the geometry of GIXRD, only structures parallel to the substrate surface can be detected.[38−40] Figure 5 shows that for low molar mass diblock copolymer thin film, $E_{76}B_{38}$, $E_{114}B_{56}$, and $E_{155}B_{76}$, no crystalline peaks of poly(oxyethylene), but a weak peak located at ~19.5° associated with (120) crystalline plane of poly(oxyethylene) is observed for high molar mass diblock copolymer, $E_{224}B_{113}$. This clearly indicates that stems of poly(oxyethylene) crystals are perpendicular to the substrate surface for low molar mass diblock copolymers, (as shown Figure 3) but parallel to the substrate surface for high molar mass diblock copolymer. In combination with AFM and GIXRD results, the nascent thin film structure of $E_{223}B_{114}$ can be illustrated in Figure 3b.

Effect of Annealing. The nascent thin film of E_mB_n block copolymers on silicon was metastable because of the two-dimensional confinement and retardation of crystallization by interaction between the block copolymer and the substrate and free surface. The block copolymer thin films were annealed 35 °C, i.e., below the crystal melting temperature, for 30 h in a vacuum system. The AFM image of annealed thin films of $E_{76}B_{38}$ is shown in Figure 6. It is found that the orientation of the lamellar structure is not qualitatively altered and is still parallel to the silicon surface. Comparing to the nascent thin film, two differences are observed for the annealed thin film. First, the irregular holes, in which there is no block copolymer on the substrate surface, basically disappear after annealing. This indicates that the E_mB_n block copolymer spreads on the silicon surface due to the preferentially interaction of poly(oxyethylene)

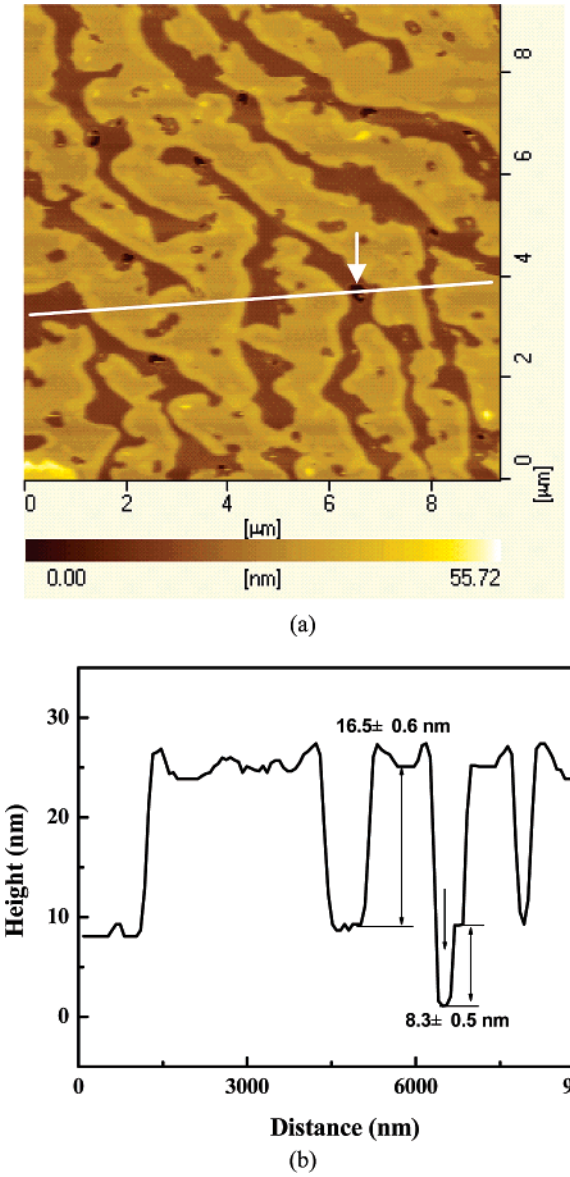

Figure 6. Tapping mode AFM height image and cross-sectional profile of annealed $E_{76}B_{38}$ thin film on silicon spin-coated from solution at concentration of 0.5% w/v: (a) height image; (b) cross-sectional profile. Annealing is performed at 35 °C for 30 h. The arrow indicates the hole throughout thin film, confirmed by the sharp difference in phase shift between silicon and polymer surfaces.

block with silicon. Second, there are no longer polymer layers with thickness $L \approx {}^1/_2L_0$ at the polymer/air interface, and only those with thickness $L \approx L_0$ are observed for the annealed thin films. This shows that the $L \approx {}^1/_2L_0$ polymer layers are metastable at the polymer/air interface and that morphological rearrangement occurs during annealing. Since disappearance of holes and the polymer layers of thickness ${}^1/_2L_0$ involves mass transportation in different polymer layers, polymers are not confined in single layers during annealing, in contrast to strongly segregated block copolymers. The structure of annealed $E_{76}B_{38}$, $E_{114}B_{56}$, and $E_{155}B_{76}$ thin films can be illustrated in Figure 3c. Similar results were obtained for the annealed $E_{114}B_{56}$ and $E_{155}B_{76}$ thin films on silicon (see Supporting Information).

Figure 7 shows AFM images of annealed $E_{224}B_{113}$ thin film. A two-dimensional spherulite structure with irregular boundaries and stripelike substructure is observed. Although the stripelike structure is observed in both nascent and annealed thin films of $E_{224}B_{113}$, in the annealed thin film all the stripes inside one

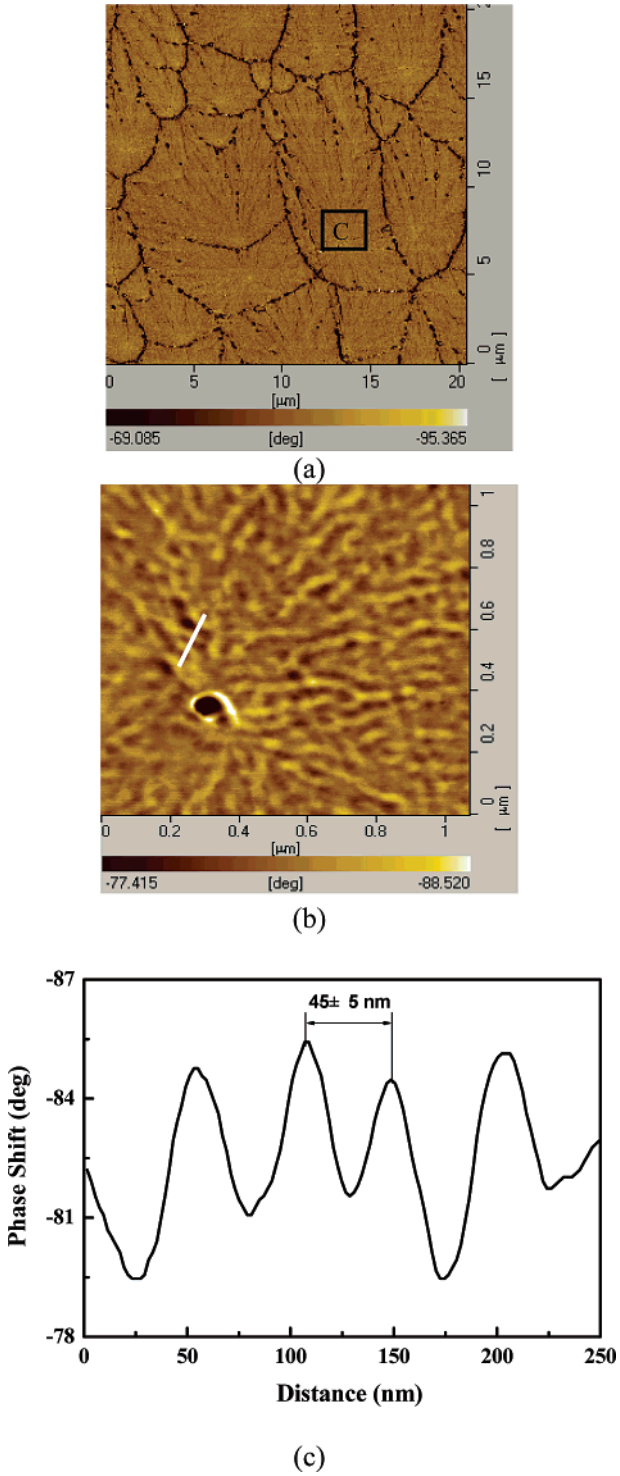

Figure 7. Tapping mode AFM phase images and cross-sectional profile of annealed $E_{224}B_{113}$ thin film on silicon spin-coated from solution at concentration of 0.5% w/v: (a) phase image; (b) phase image with higher magnification; (c) cross-sectional profile along the line in (b). Annealing is performed at 35 °C for 30 h.

spherulite radiate from a common center, whereas this is not the case of the nascent thin film. An image at higher magnification (Figure 7b) reveals that the common center of the stripes inside a spherulite is a heterogeneity on the silicon surface. This observation clearly shows that the heterogeneities on the substrate can nucleate secondary crystallization of $E_{224}B_{113}$ thin film during annealing. In contrast, it has been reported that crystallization of thin film with lamellar structure parallel to the surface of substrate is nucleated by the preexisting holes.[17,18]

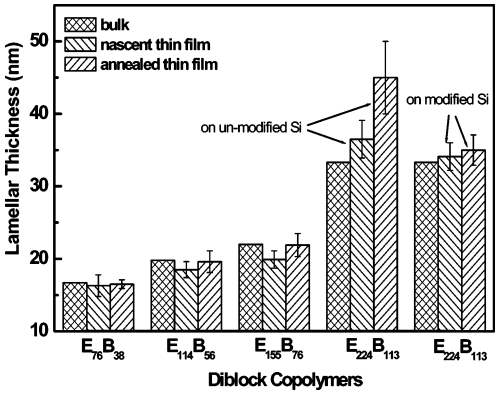

Figure 8. Lamellar thickness of E_mB_n diblock copolymers in bulk, nascent thin films, and annealed thin films.

Figure 8 shows histograms of the lamellar thicknesses of nascent and annealed thin films compared to the long period in bulk. It is observed that for shorter E_mB_n block copolymers ($E_{76}B_{38}$, $E_{114}B_{56}$, and $E_{155}B_{76}$), which have structures parallel to the substrate surface, the lamellar thickness of the nascent film is slightly smaller than the long period in bulk. This difference becomes larger with increasing chain length. This is possibly due to lower crystallinity of the nascent thin film. For long block copolymer such as $E_{155}B_{76}$, the stronger segregation strength may also retard crystallization. After a long annealing time, however, the crystallinity of the E block is increased and the amorphous B block becomes more stretched accordingly. As a result, the lamellar thickness becomes slightly larger after annealing and is comparable that of the bulk. In contrast, for $E_{224}B_{113}$, both the nascent and the annealed thin films have evidently larger lamellar thickness than the long period in the bulk. There are two potential explanations for this. (1) The poly(oxyethylene) crystals are not arranged in a perfectly parallel way, and especially in the annealed thin film there are lots of branches in the stripes. (2) The height profiles of the nascent and annealed $E_{224}B_{113}$ thin films on silicon (see Supporting Information) reveal that the thin films undulate within several nanometers, which makes the block copolymer a little more extended. Both situations result in a larger lamellar thickness than the long period in the bulk.

Effect of Substrate Surface Modification. Surface energy of the substrate has a pronounced effect on thin film morphology, a situation that is well characterized for amorphous block copolymers[41−44] in terms of theory and experiment. For example, lamellar structures parallel to the substrate surface are favorably formed when the substrate preferably absorbs one of the components, while lamellar structure perpendicular to the substrate surface is favorable for neutral substrates. In the present work, a monolayer of organic molecule was grafted onto the silicon surface, and the effect of surface property on thin film morphology was investigated. Trimethylchlorosilane, a grafting agent with single functional group, was selected to ensure a monolayer of methylsilane groups on the silicon surface, as shown in Figure 9. The water contact angle method is used to determine the modification effect. The water contact angle of modified silicon was determined to be 84.8°, being ~56° higher than that of the initial hydrophilic silicon substrate (28.4°). The modified silicon surface is hydrophobic, and hence E blockphobic, compared to the initial silicon surface due to formation of monolayer of silane molecules on the silicon.

Figure 10 shows the AFM image of a nascent $E_{224}E_{113}$ thin film on hydrophobically modified silicon. It is found that there is a periodicity in the direction perpendicular to the silicon surface. An image at higher magnification shows no ordered structure within the polymer layers. From this observation we can draw the conclusion that the lamellar structures of nascent thin films of $E_{224}E_{113}$ on hydrophobically modified silicon are parallel to the silicon surface. In contrast, the nascent $E_{224}E_{113}$ thin film on an unmodified hydrophilic silicon surface has a perpendicular lamellar structure. As a result, reduction of hydrophilicity of the substrate surface can lead to the change of orientation of lamellar structure. From the cross-sectional profile, the thickness of the polymer layers is an integeral repeat of the long period of $E_{224}B_{113}$ in the bulk, and there are no polymer layers with thickness of $L_0/2$ near the holes. This further demonstrates that modified silicon surface tends to absorb preferably hydrophobic B segments, and the structure of $E_{224}B_{113}$

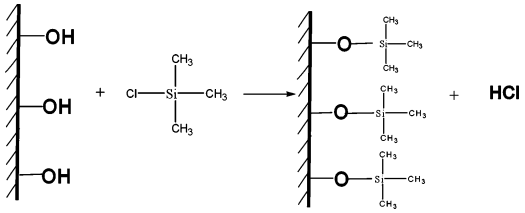

Figure 9. Scheme for surface modification of silicon wafer using trimethylchlorosilane as grafting agent.

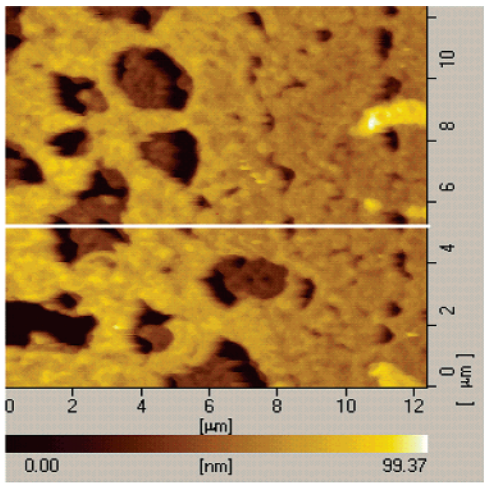

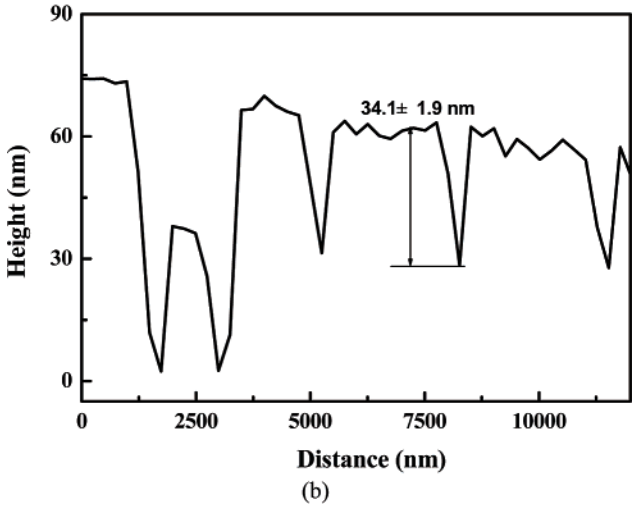

Figure 10. Tapping mode AFM height image and cross-sectional profile of nascent $E_{224}B_{113}$ thin film on modified silicon spin-coated from solution at concentration of 0.5% w/v: (a) height image; (b) cross-sectional profile.

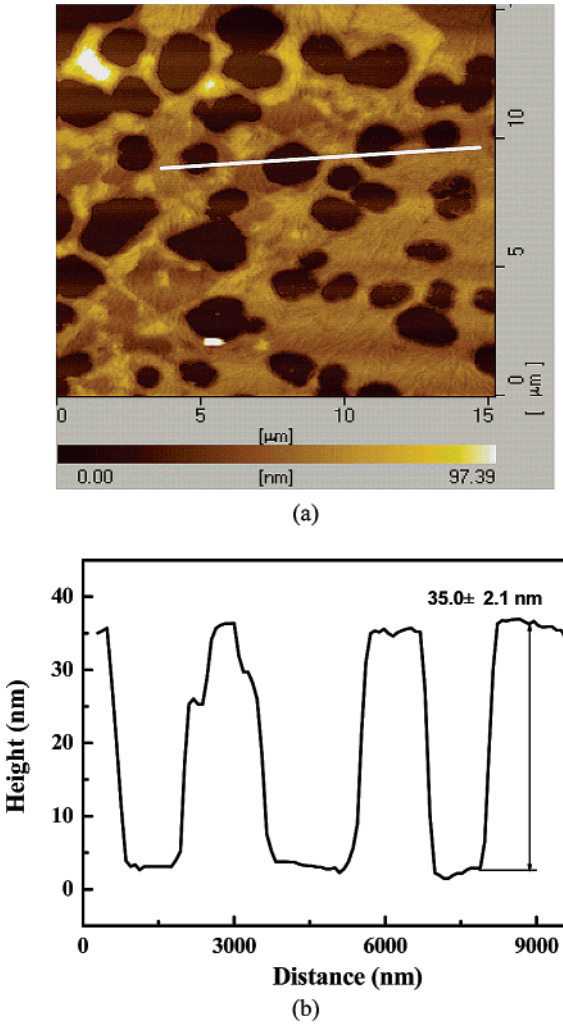

Figure 11. Tapping mode AFM height image and cross-sectional profile of annealed $E_{224}B_{113}$ thin film on modified silicon spin-coated from solution at concentration of 0.5% w/v: (a) height image; (b) cross-sectional profile. Annealing is performed at 35 °C for 30 h.

on the modified silicon surface can be schematically depicted in Figure 3d.

Figure 11 shows the AFM image of $E_{224}E_{113}$ thin film on modified silicon after annealing at 35 °C for 30 h. It is observed that dewetting takes place during annealing. The thickness of the annealed thin film is slightly larger than the long period in the bulk. As a result, we believe that lamellar structure of the thin film remains parallel to the surface after annealing. Comparing Figure 11 with Figure 7, it is clear that the structure of annealed $E_{224}B_{113}$ thin film of on hydrophobically modified silicon is qualitatively different from the spherulite structure of annealed $E_{224}B_{113}$ on a hydrophilic silicon surface and is similar to the structure reported for weakly segregated polystyrene-*b*-polycaprolactone block copolymer with a parallel orientation to the substrate surface, in which crystallization is nucleated by the stretched polycaprolactone at the edge of holes.[17,18] We speculate that the nucleation of crystallization in block copolymer thin film depends on the orientation of the lamellar structure. Only when the melt lamellar structure is perpendicular to the substrate surface can surface heterogeneities act as nuclei for crystallization. When the lamellar structure is parallel to the substrate surface, the nucleation effect of the heterogeneities on the silicon surface is screened due to the absorption of amorphous poly(oxybutylene) block at the first layer nearest to the substrate.

Conclusions

The above results show that semicrystalline E_mB_n block copolymers can exhibit abundant morphologies in the thin film supported on silicon, depending on chain length, thermal history, and substrate surface property. The nascent thin films of low molar mass block copolymers ($E_{76}B_{38}$, $E_{114}B_{56}$, and $E_{155}B_{76}$) show the lamellar structure parallel to the substrate surface, but the high molar mass block copolymer, $E_{224}B_{113}$, exhibits the lamellar orientation perpendicular to the substrate surface. The nascent thin films of low molar mass block copolymers are composed of multiple polymer layers and have mixed thickness $L \approx L_0$ and $L \approx L_0/2$ (L_0, the long period of the block copolymers in the bulk) besides the polymer layer nearest to the substrate. As a result, it can be identified that the crystalline domain in the block copolymers consists of double poly(oxyethylene) layers. Annealing leads to the disappearance of the metastable polymer layer of thickness $L \approx L_0/2$, morphological transformation involving different polymer layers, and slight increase in lamellar thickness. The heterogeneities on the substrate surface can nucleate crystallization of block copolymer thin film during annealing when the lamellar structure is perpendicular to the surface, leading to spherulite morphology. When the silicon surface was modified by a monolayer of silane molecules, the surface becomes hydrophobic and tends to absorb preferentially the amorphous poly(oxybutylene) block. On the modified silicon surface, the lamellar structure of $E_{224}B_{113}$ becomes parallel to the surface, and the nucleation effect of the heterogeneities on crystallization of poly(oxyethylene) block is shielded.

Acknowledgment. This research was supported by ICI and the National Natural Science Foundation of China (20374046), the Excellent Young Teachers Program, and New Century Supporting Program for the Talents by the Chinese Ministry of Education.

Supporting Information Available: Height AFM images of nascent and annealed $E_{114}B_{56}$, $E_{155}B_{76}$, and $E_{224}B_{113}$ and corresponding cross-sectional profiles. This material is available free of charge via the Internet at http://pubs.acs.org.

References and Notes

(1) Fasolka, M. J.; Mayes, A. M. *Annu. Rev. Mater. Res.* **2001**, *31*, 323.
(2) Green, P. F. *J. Polym. Sci., Part B: Polym. Phys.* **2003**, *41*, 2219.
(3) Green, P. F.; Limary, R. *Adv. Colloid Interface Sci.* **2001**, *94*, 53.
(4) Segalman, R. A. *Mater. Sci. Eng., R* **2005**, *48*, 191.
(5) Balsamo, V.; Collins, S.; Hamley, I. W. *Polymer* **2002**, *43*, 4207.
(6) Li, Y.; Loo, Y. L.; Register, R. A.; Green, P. F. *Macromolecules* **2005**, *38*, 7745.
(7) Lambreva, D. M.; Opitz, R.; Reiter, G.; Frederik, P. M.; de Jeu, W. H. *Polymer* **2005**, *46*, 4868.
(8) Reiter, G.; Castelein, G.; Sommer, J. U. *Macromol. Symp.* **2002,** *183*, 173.
(9) Reiter, G.; Castelein, G.; Hoerner, P.; Riess, G.; Blumen, A.; Sommer, J. U. *Phys. Rev. Lett.* **1999**, *83*, 3844.
(10) Opitz, R.; Lambreva, D. M.; de Jeu, W. H. *Macromolecules* **2002**, *35*, 6930.
(11) Park, C.; De Rosa, C.; Lotz, B.; Fetters, L. J.; Thomas, E. L. *Macromol. Chem. Phys.* **2003**, *204*, 1514.
(12) De Rosa, C.; Park, C.; Thomas, E. L.; Lotz, B. *Nature (London)* **2000**, *405*, 433.
(13) Park, C.; De Rosa, C.; Thomas, E. L. *Macromolecules* **2001**, *34*, 2602.
(14) Hong, S.; MacKnight, W. J.; Russell, T. P.; Gido, S. P. *Macromolecules* **2001**, *34*, 2876.
(15) Hong, S.; MacKnight, W. J.; Russell, T. P.; Gido, S. P. *Macromolecules* **2001**, *34*, 2398.
(16) De Rosa, C.; Park, C.; Lotz, B.; Wittmann, J. C.; Fetters, L. J.; Thomas, E. L. *Macromolecules* **2000**, *33*, 4871.
(17) Zhang, F. J.; Chen, Y. Z.; Huang, H. Y.; Hu, Z. J.; He, T. B. *Langmuir* **2003**, *19*, 5563.

(18) Zhang, F. J.; Huang, H. Y.; Hu, Z. J.; Chen, Y. Z.; He, T. B. *Langmuir* **2003**, *19*, 10100.
(19) Fu, J.; Cong, Y.; Li, J.; Luan, B.; Pan, C. Y.; Yang, Y. M.; Li, B. Y.; Han, Y. C. *Macromolecules* **2004**, *37*, 6918.
(20) Vasilev, C.; Heinzelmann, H.; Reiter, G. *J. Polym. Sci., Part B: Polym. Phys.* **2004**, *42*, 1312.
(21) Rottele, A.; Thurn-Albrecht, T.; Sommer, J. U.; Reiter, G. *Macromolecules* **2003**, *36*, 1257.
(22) Li, X.; Han, Y. C.; An, L. J. *Langmuir* **2002**, *18*, 5293.
(23) Fu, J.; Luan, B.; Yu, X.; Cong, Y.; Li, J.; Pan, C. Y.; Han, Y. C.; Yang, Y. M.; Li, B. Y. *Macromolecules* **2004**, *37*, 976.
(24) Fu, J.; Luan, B.; Pan, C. Y.; Li, B. Y.; Han, Y. C. *Macromolecules* **2005**, *38*, 5118.
(25) Reiter, G. *J. Polym. Sci., Part B: Polym. Phys.* **2003**, *41*, 1869.
(26) Lotz, B.; Kovacs, A. J. *Kolloid Z. Z. Polym.* **1966**, *209*, 97.
(27) Lotz, B.; Kovacs, A. J.; Bassett, G. A.; Keller, A. *Kolloid Z. Z. Polym.* **1966**, *209*, 115.
(28) Reiter, G.; Castelein, G.; Hoerner, P.; Riess, G.; Sommer, J. U.; Floudas, G. *Eur. Phys. J. E* **2000**, *2*, 319.
(29) Loo, Y. L.; Register, R. A.; Ryan, A. J. *Macromolecules* **2002**, *35*, 2365.
(30) Xu, J. T.; Fairclough, J. P. A.; Mai, S. M.; Ryan, A. J.; Chaibundit, C. *Macromolecules* **2002**, *35*, 6937.
(31) Busch, P.; Posselt, D.; Smilgies, D. M.; Rheinlander, B.; Kremer, F.; Papadakis, C. M. *Macromolecules* **2003**, *36*, 8717.
(32) Reiter, G.; Castelein, G.; Sommer, J. U.; Rottele, A.; Thurn-Albrecht, T. *Phys. Rev. Lett.* **2001,** *87*, 6101.
(33) Mai, S. M.; Fairclough, J. P. A.; Viras, K.; Gorry, P. A.; Hamley, I. W.; Ryan, A. J.; Booth, C. *Macromolecules* **1997,** *30*, 8392.
(34) Mai, S. M.; Fairclough, J. P. A.; Terrill, N. J.; Turner, S. C.; Hamley, I. W.; Matsen, M. W.; Ryan, A. J.; Booth, C. *Macromolecules* **1998**, *31*, 8110.
(35) Ryan, A. J.; Mai, S. M.; Fairclough, J. P. A.; Hamley, I. W.; Booth, C. *Phys. Chem. Chem. Phys.* **2001,** *3*, 2961.
(36) Hamley, I. W.; Wallwork, M. L.; Smith, D. A.; Fairclough, J. P. A.; Ryan, A. J.; Mai, S. M.; Yang, Y. W.; Booth, C. *Polymer* **1998,** *39*, 3321.
(37) Xu, J. T.; Turner, S. C.; Fairclough, J. P. A.; Mai, S. M.; Ryan, A. J.; Chaibundit, C.; Booth, C. *Macromolecules* **2002**, *35*, 3614.
(38) Durell, M.; Macdonald, J. E.; Trolley, D.; Wehrum, A.; Jukes, P. C.; Jones, R. A. L.; Walker, C. J.; Brown, S. *Europhys. Lett.* **2002**, *58*, 844.
(39) Murthy, N. S.; Bednarczyk, C.; Minor, H. *Polymer* **2000**, *41*, 277.
(40) Lee, B.; Park, I.; Yoon, J.; Park, S.; Kim, J.; Kim, K. W.; Chang, T.; Ree, M. *Macromolecules* **2005**, *38*, 4311.
(41) Huang, E.; Russell, T. P.; Harrison, C.; Chaikin, P. M.; Register, R. A.; Hawker, C. J.; Mays, J. *Macromolecules* **1998**, *31*, 7641.
(42) Huang, E.; Pruzinsky, S.; Russell, T. P.; Mays, J.; Hawker, C. J. *Macromolecules* **1999**, *32*, 5299.
(43) Huang, E.; Mansky, P.; Russell, T. P.; Harrison, C.; Chaikin, P. M.; Register, R. A.; Hawker, C. J.; Mays, J. *Macromolecules* **2000**, *33*, 80.
(44) Mansky, P.; Russell, T. P.; Hawker, C. J.; Pitsikalis, M.; Mays, J. *Macromolecules* **1997**, *30*, 6810.

MA060405P